Electronic Supplementary Information

Introducing of proton/electron mediators enhances catalytic ability of iron porphyrin complex for photochemical CO_2 reduction

Maho Imai,[a†] Kento Kosugi,[a†] Yutaka Saga,[a] Mio Kondo,[*abc] and Shigeyuki Masaoka[*ab]

[a]Division of Applied Chemistry, Graduate School of Engineering, Osaka University, 2-1 Yamadaoka, Suita, Osaka 565-0871, Japan

[b]Innovative Catalysis Science Division, Institute for Open and Transdisciplinary Research Initiatives (ICS-OTRI), Osaka University, Suita, Osaka 565-0871, Japan

[c]PRESTO, Japan Science and Technology Agency (JST), 4-1-8 Honcho, Kawaguchi, Saitama 332-0012, Japan

[†]These authors contributed equally.

Table of contents

1. Experimental details 3

General procedures 3

Syntheses 3

Photochemistry 17

$^{13}CO_2$ labeling experiment 17

Electrochemistry 17

2. UV-vis absorption spectroscopy 18

3. Electrochemical measurements 19

4. Photocatalytic activity for CO_2 reduction 20

5. Quantum chemical calculation 22

6. Emission quenching experiments 23

7. Comparison of catalytic ability 24

8. References 27

1. Experimental details

General procedures

Pyrrole, boron trifluoride diethyl etherate ($BF_3 \cdot OEt_2$) and sodium borohydride were purchased from Sigma-Aldrich Co., LLC. Propanoic acid was purchased from Kishida Chemical Co., LLC. Benzaldehyde, Triethylamine (TEA), sodium sulfate (Na_2SO_4), sodium dithionite ($Na_2S_2O_4$), 2 M hydrochloric acid, sodium chloride, toluene, pyridinium chloride, ethyl acetate (EtOAc), tris(2-phenylpyridinato)iridium(III) ($Ir(ppy)_3$), potassium hydroxide and iron(II) chloride tetrahydrate ($FeCl_2 \cdot 4H_2O$) was purchased from Wako Pure Chemical Industries, Ltd. Sodium hydrogen carbonate ($NaHCO_3$), iron(III) chloride ($FeCl_3$), methanol (MeOH), acetone, ethanol (EtOH), *N,N*-dimethylformamide (DMF), tetrahydrofuran (THF), chloroform ($CHCl_3$) and acetonitrile (MeCN) were purchased from Kanto Chemical Co., Inc. Acetone-d_6, acetonitrile-d_3 and chloroform-*d* were purchased from Cambridge Isotopes, Inc. 2,6-lutidine, 2,3-dichloro-5,6-dicyano-p-benzoquinone (DDQ), tetra-*n*-butylammonium perchlorate (TBAP), iodomethane, 2,5-dimethoxybenzaldehyde, 2,6-dimethoxybenzaldehyde, 1,8-diazabicyclo[5.4.0]-7-undecene (DBU) and 2,2,2-trifluoroethanol (TFE) were purchased from Tokyo Chemical Industry Co., Ltd. 2-phenylbenzimidazole was purchased from Combi-Blocks, Inc. All solvents and reagents are of the highest quality available and used as received except for TBAP. TBAP was recrystallized from EtOH/H_2O. H_2O was purified using a Millipore MilliQ purifier. ^1H-NMR and ^{13}C-NMR spectra were collected at room temperature on a JEOL JNM-ECS400 spectrometer. Elemental analysis was performed on a J-SCIENCE LAB MICRO CORDER JM10 elemental analyzer. MALDI spiral-TOF mass spectra were measured on a JMS-S3000 mass spectrometer. UV-visible absorption spectra were recorded on a UV-Vis Agilent Cary8454 spectrophotometer and a Shimadzu UV-3600 UV-vis-near-IR spectrophotometer. Fluorescence emission spectra were recorded on a SHIMADZU RF-5300PC.

Syntheses

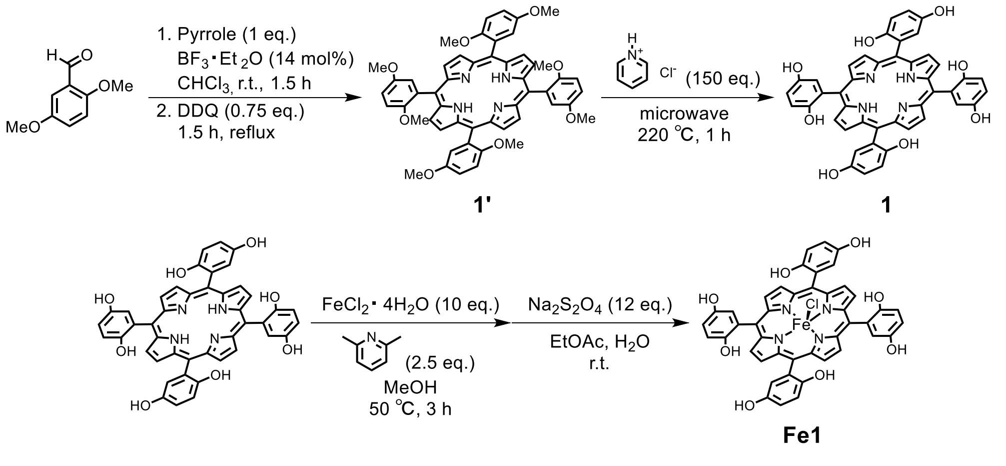

Scheme S1. Synthetic scheme for **Fe1**.

Synthesis of 5,10,15,20-tetrakis(2,5-dimethoxyphenyl)porphyrin (1')

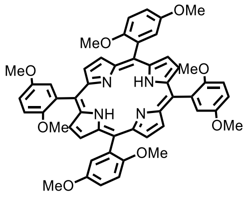

1' was synthesized by the modification of a previous report.[S1] 2,5-dimethoxybenzaldehyde (1.01 g, 6.08 mmol) was dissolved in $CHCl_3$ (600 mL), then stirred for 20 min under N_2 atmosphere. After pyrrole (0.45 mL, 6.4 mmol) was added, boron trifluoride diethyl etherate ($BF_3 \cdot OEt_2$) (0.25 mL, 0.95 mmol) was added to the reaction mixture, and the mixture was stirred for 1.5 h at room temperature in the dark. Subsequently, a solution of DDQ (1.05 g, 4.64 mmol) in toluene (20 mL) was added, and the mixture was refluxed. After 1.5 h, the reaction mixture was quenched by TEA (0.50 mL, 3.6 mmol). The resulting mixture was purified by silica gel column chromatography ($CHCl_3$ as eluent) to afford a dark purple solution. Recrystallization from $CHCl_3$/MeOH gave a purple solid of **1'** (243 mg, yield 19%). ^{1}H-NMR (400 MHz, acetone-d_6) δ 8.80 (d, J = 2.2 Hz, 8H), 7.65 (td, J = 18.9, 2.2 Hz, 4H), 7.41 (m, 8H), 3.94 (t, J = 3.2 Hz, 12H), 3.55 (t, J = 3.7 Hz, 12H), −2.65 (brs, 2H) ppm. ^{13}C-NMR (400 MHz, chloroform-d): δ = 154.20, 154.13, 152.33, 132.13, 132.07, 130.66, 121.35, 121.28, 115.29, 114.77, 112.48, 112.43, 112.22, 56.78, 56.72, 55.92. HRMS (MALDI): m/z Calcd. for $C_{52}H_{46}N_4O_8$ $[M]^+$ 854.33102. Found 854.32859. Elemental analysis Calcd. for $C_{52}H_{47.5}N_4O_{8.75}$ (**1'**$\cdot$0.75 H_2O): C, 71.92%; H, 5.51%; N, 6.45%. Found: C, 71.82%; H, 5.38%; N, 6.44%. Note that multiple peaks in ^{13}C NMR spectrum of **1'** are due to the presence of atropisomers.

Synthesis of 5,10,15,20-tetrakis(2,5-dihydroxyphenyl)porphyrin (1)

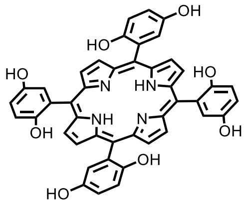

1 was synthesized by the modification of a previous report.[S2] To a microwave vessel, **1'** (101 mg, 0.118 mmol) and pyridinium chloride (2.07 g, 17.9 mmol) were added. The reaction mixture was heated at 220 °C by a microwave reactor. After 1 h, the resulting mixture was dissolved in water and $NaHCO_3$ was added until pH was neutral. The resulting mixture was extracted with EtOAc. Then, the extract was washed with brine, and dried over anhydrous Na_2SO_4, and concentrated under reduced pressure. The resulting mixture was purified by silica gel column chromatography ($CHCl_3$/MeOH = 1/0 to 3/1) to afford **1** as a purple solid (57.5 mg, yield 65%). ^{1}H-NMR (400 MHz, acetonitrile-d_3) δ 8.87 (s, 8H), 7.43 (m, 4H), 7.12-7.18 (m, 8H), 6.87 (brs, 4H), 6.32-6.40 (m, 4H), −2.85 (brs, 2H) ppm. ^{13}C-NMR (400 MHz, methanol-d_4): δ = 151.75, 150.34, 130.84, 123.46, 117.70, 117.28, 117.19. HRMS (MALDI): m/z Calcd. for $C_{44}H_{31}N_4O_8$ $[M + H^+]^+$

743.21364. Found 743.21052.

Insertion of an iron ion into 1

Insertion of an iron ion into **1** was carried out following the modification of a previous report.[S1] A solution of **1** (46.1 mg, 0.0621 mmol), $FeCl_2 \cdot 4H_2O$ (122 mg, 0.611 mmol) and 2,6-lutidine (17.7 µL, 0.152 mmol) was heated at 50 °C and stirred for 3 h under Ar atmosphere in MeOH (15 mL). After MeOH was removed, the resulting solid was dissolved in EtOAc, washed with water and brine. The solution was dried over anhydrous Na_2SO_4 and concentrated under reduced pressure. Then, the resulting solid was washed with $CHCl_3$ and the brown solid was obtained (38.7 mg, without further purification).

Reduction to 5,10,15,20-tetrakis(2,5-dihydroxyphenyl)porphyrinato iron(III) chloride (Fe1)

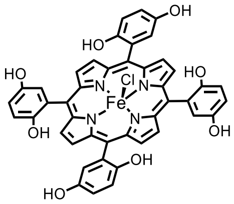

To reduce oxidized hydroquinone moieties, a solution of the resulting solid (21.0 mg) and $Na_2S_2O_4$ (53.3 mg, 0.306 mmol) in EtOAc (10 mL) and water (10 mL) was bubbled by Ar gas for 30 minutes. After 30 minutes, the organic layer was washed with saturated aqueous $NaHCO_3$ solution. To the solution, 1 M HCl was added, then bubbled by Ar gas for 5 minutes. After 5 minutes, the organic layer was washed with brine, and hexane was added to the solution. Precipitate was collected by filtration. The brown solid of **Fe1** was obtained (15.3 mg). HRMS (MALDI): *m/z* Calcd. for $C_{44}H_{28}N_4O_8Fe$ $[M - Cl]^+$ 796.12511. Found 796.12817. Elemental analysis Calcd. for $C_{44}H_{36}ClFeN_4O_{12}$ (**Fe1**$\cdot$4.00 H_2O): C, 58.45%; H, 4.01%; N, 6.20%. Found: C, 58.49%; H, 4.03%; N, 6.10%.

Synthesis of 5,10,15,20-tetrakis(2,6-dimethoxyphenyl)porphyrin (H_2TDMPP)

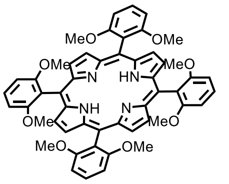

H_2TDMPP was synthesized by the modification of a previous report.[S1] 2,6-dimethoxybenzaldehyde (1.04 g, 6.26 mmol) was dissolved in $CHCl_3$ (600 mL), then stirred for 20 min under N_2 atmosphere. After pyrrole (0.45 mL, 6.4 mmol) was added, boron trifluoride diethyl etherate ($BF_3 \cdot OEt_2$) (0.22 mL, 0.84 mmol) was added to the reaction mixture, and the mixture was stirred for 1.5 h at room temperature in the dark. Subsequently, a solution of DDQ (1.03 g, 4.51 mmol) in toluene (20 mL) was added, and the mixture was refluxed. After 1.5 h, the reaction mixture was quenched by TEA (0.50 mL, 3.6 mmol). The resulting mixture was purified by silica gel column chromatography ($CHCl_3$ as eluent) to afford a dark purple solution. Recrystallization from $CHCl_3$/MeOH gave a purple solid of **H_2TDMPP** (297 mg, yield 22%). ^{1}H-NMR (400 MHz, chloroform-*d*) δ 8.67 (s, 8H), 7.68 (t, J = 8.5 Hz, 4H), 6.97 (d, *J* = 8.3 Hz, 8H), 3.50 (s, 24H), −2.50 (brs, 2H) ppm. ^{13}C-NMR (400 MHz, chloroform-*d*): δ = 160.67, 129.78, 120.53, 110.70, 104.31, 56.12. HRMS (MALDI): *m/z* Calcd. for $C_{52}H_{46}N_4O_8$ $[M]^+$ 854.33102. Found 854.32874.

Synthesis of 5,10,15,20-tetrakis(2,6-dihydroxyphenyl)porphyrin (H_2TDHPP)

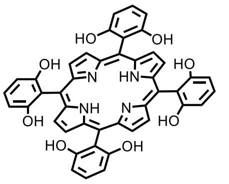

H_2TDHPP was synthesized by the modification of a previous report.[S2] To a microwave vessel, **H_2TDMPP** (100 mg, 0.117 mmol) and pyridinium chloride (2.24 g, 19.4 mmol) were added. The reaction mixture was heated at 220 °C by a microwave reactor. After 3 h, the resulting mixture was dissolved in water and $NaHCO_3$ was added until pH was neutral. The resulting mixture was extracted with EtOAc, then the extract was washed with brine, and dried over anhydrous Na_2SO_4, and concentrated under reduced pressure. The resulting mixture was purified by silica gel column chromatography ($CHCl_3$/MeOH = 10/1 to 5/1) to afford **H_2TDHPP** as a purple solid (25.7 mg, yield 30%). ^{1}H-NMR (400 MHz, acetonitrile-*d*$_3$) δ 8.83 (s, 8H), 7.54 (t, *J* = 8.3 Hz, 4H), 6.87 (d, *J* = 8.2 Hz, 8H), 6.76 (s, 8H), −2.74 (brs, 2H) ppm. ^{13}C-NMR (400 MHz, methanol-*d*$_4$): δ = 159.68, 131.28, 118.22, 112.57, 108.10. HRMS (MALDI): *m/z* Calcd. for $C_{44}H_{30}N_4O_8$ $[M]^+$ 742.20582. Found 742.20520.

Synthesis of 5,10,15,20-tetrakis(2,6-dihydroxyphenyl)porphyrinato iron(III) chloride (CAT)

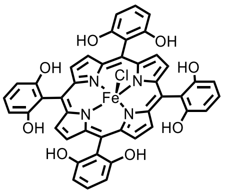

CAT was synthesized by the modification of a previous report.[S1] A solution of **H_2TDHPP** (22.0 mg, 0.0296 mmol), $FeCl_2 \cdot 4H_2O$ (53.8 mg, 0.271 mmol) and 2,6-lutidine (7.9 µL, 0.068 mmol) was heated at 50 °C and stirred for 3 h under Ar atmosphere in MeOH (10 mL). After MeOH was removed, the resulting solid was dissolved in EtOAc, and 1 M HCl was added. After 30 min stirring, the organic layer was washed with brine. After removing the solvent, the black solid of **CAT** was obtained (3.4 mg, yield 14%). HRMS (MALDI): *m/z* Calcd. for $C_{44}H_{28}N_4O_8Fe$ $[M - Cl]^+$ 796.12511. Found 796.12535. Elemental analysis Calcd. for $C_{44}H_{41}ClFeN_4O_{14.5}$ (**CAT**·6.50 H_2O): C, 55.68%; H, 4.35%; N, 5.90%. Found: C, 55.76%; H, 4.20%; N, 5.71%.

Synthesis of tetraphenylporphyrin (H_2TPP)

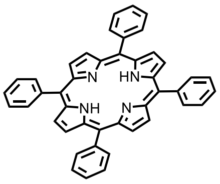

H_2TPP was prepared as previously described.[S3] Pyrrole (1.7 mL, 25 mmol) and benzaldehyde (2.6 mL, 25 mmol) were dissolved in propanoic acid (50 mL), then refluxed for 45 minutes and cooled to room temperature. The resulting mixture was filtered and washed with methanol. Recrystallization from $CHCl_3$/methanol gave a purple solid (785 mg, yield 20%). ^{1}H-NMR (400 MHz, chloroform-*d*): δ = 8.82 (s, 8H), 8.19-8.21 (m, 8H), 7.71-7.78 (m, 12H), –2.80 (s, 2H) ppm. ^{13}C NMR (400 MHz, chloroform-*d*): δ = 142.15, 134.56, 127.70, 126.69, 120.13. HRMS (MALDI): *m/z* Calcd. for $C_{40}H_{30}N_4$ $[M]^+$ 614.24650. Found 614.24591. Elemental analysis Calcd. for $C_{44}H_{30.5}N_4O_{0.25}$ (**H_2TPP**·0.25 H_2O): C, 85.34%; H, 4.96%; N, 9.05%. Found: C, 85.24%; H, 4.68%; N, 9.08%.

Synthesis of 5,10,15,20-tetrakis(phenyl)porphyrinato iron(III) chloride (FeTPP-Cl)

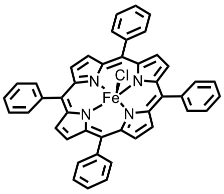

FeTPP-Cl was prepared by the modification of a previous report.[S4] To a solution of **H_2TPP** (200 mg, 0.325 mmol) in DMF (10 mL), a DMF 10 mL solution of $FeCl_3$ (519 mg, 3.20 mmol) was added at room temperature. The mixture was heated at 200 ˚C for 1 h by a microwave reactor. Diluted HCl (1 M, 50 mL) was added to the resulting solution. Precipitate was collected by filtration and washed with 1 M HCl. Recrystallization from $CHCl_3$/hexane gave a purple solid (191 mg, yield 85%). HRMS (MALDI): *m/z* Calcd. for $C_{44}H_{28}N_4Fe$ $[M - Cl]^+$ 668.16579. Found 668.16517. Elemental analysis Calcd. for $C_{44}H_{28}ClFeN_4$ (**FeTPP-Cl**): C, 75.06%; H, 4.01%; N, 7.96%. Found: C, 74.98%; H, 4.08%; N, 8.01%.

Synthesis of 1,3-dimethyl-2-phenyl-2,3-dihydro-1*H*-benzo[*d*]imidazole (BIH)

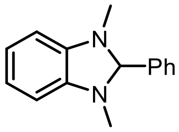

BIH was synthesized as previously reported.[S5] ^{1}H-NMR (400 MHz, acetonitrile-d_3): δ 7.58–7.55 (m, 2H), 7.46-7.44 (m, 3H), 6.66 (dd, *J* = 3.2, 5.5 Hz, 2H), 6.45 (dd, J = 3.2, 5.5 Hz, 2H), 4.85 (s, 1H), 2.51 (s, 6H) ppm. ^{13}C-NMR (400 MHz, chloroform-*d*): δ = 142.04, 139.00, 129.30, 128.82, 128.43, 119.27, 105.70, 93.97, 33.14. HRMS (MALDI): *m/z* Calcd. for $C_{15}H_{15}N_2$ $[M - H]^+$ 223.12297. Found 233.12406.

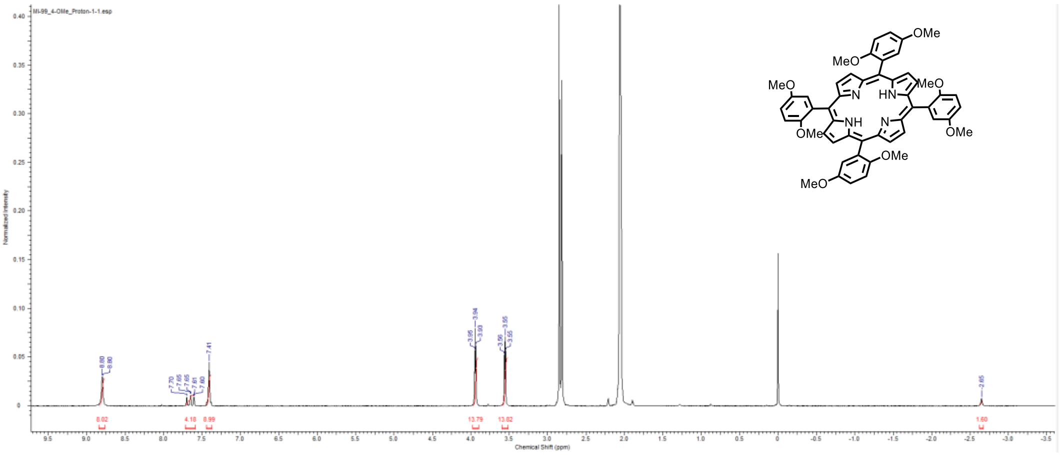

Fig. S1 ^{1}H NMR spectrum of **1’** in acetone-d_6.

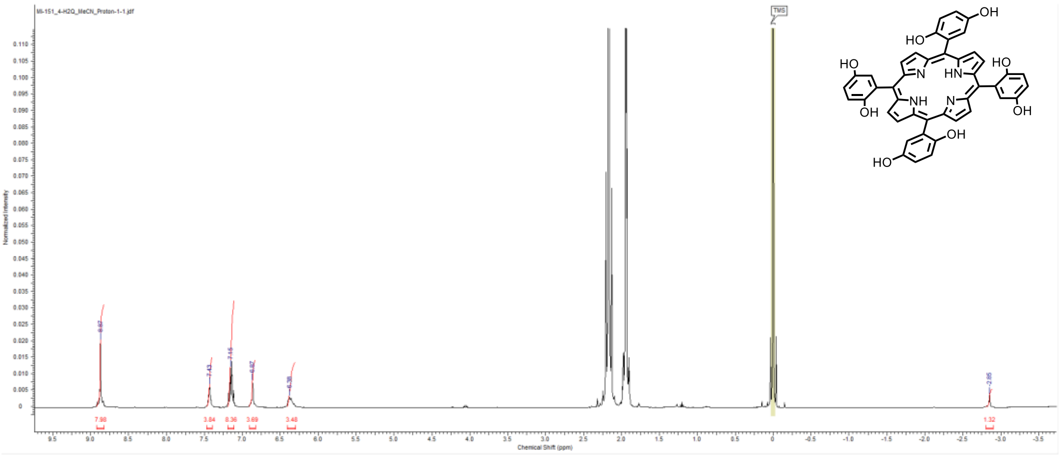

Fig. S2 ^{1}H NMR spectrum of **1** in acetonitrile-*d*$_3$.

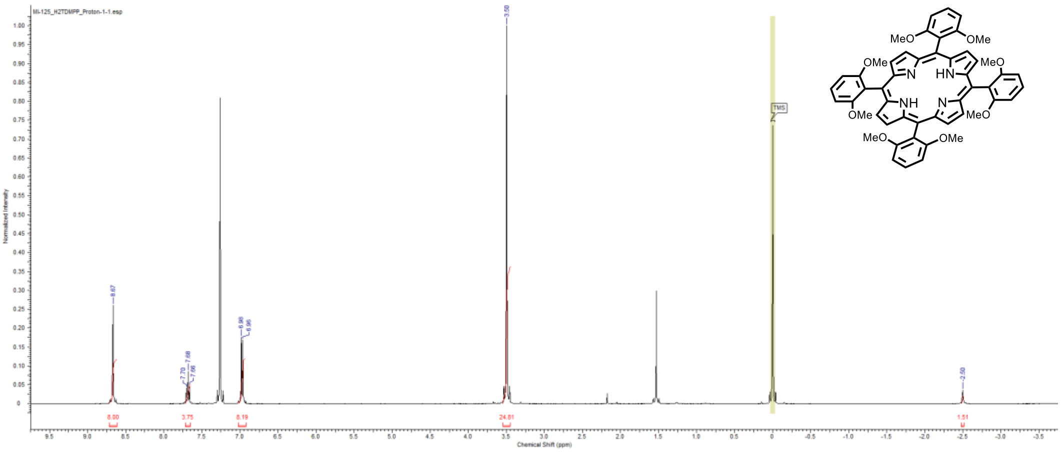

Fig. S3 ^{1}H NMR spectrum of **H$_2$TDMPP** in chloroform-*d*.

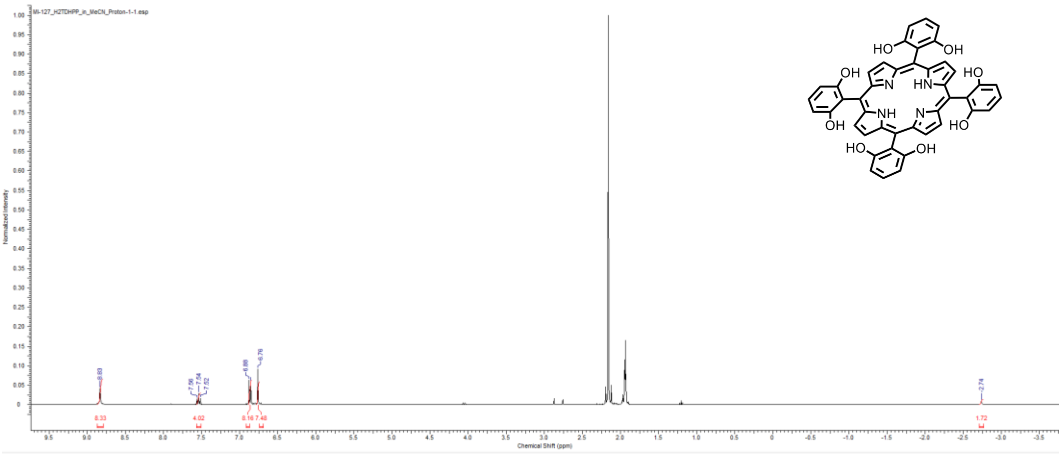

Fig. S4 ^{1}H NMR spectrum of **H$_2$TDHPP** in methanol-*d*$_4$.

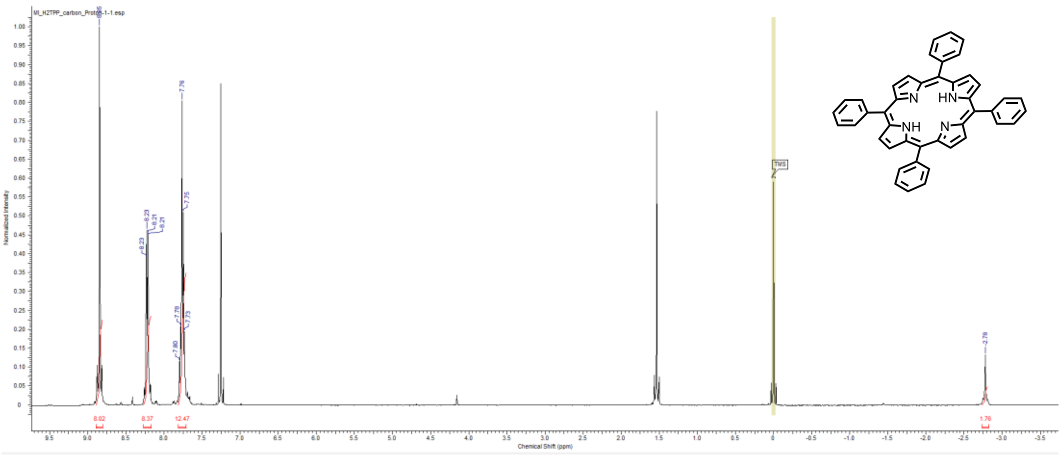

Fig. S5 ^{1}H NMR spectrum of **H_2TPP** in chloroform-*d*.

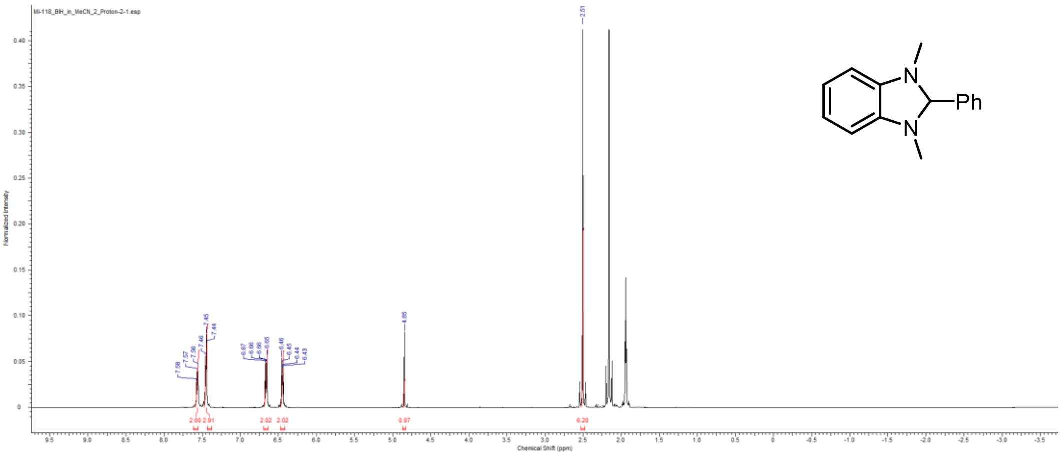

Fig. S6 ^{1}H NMR spectrum of BIH in acetonitrile-d_3.

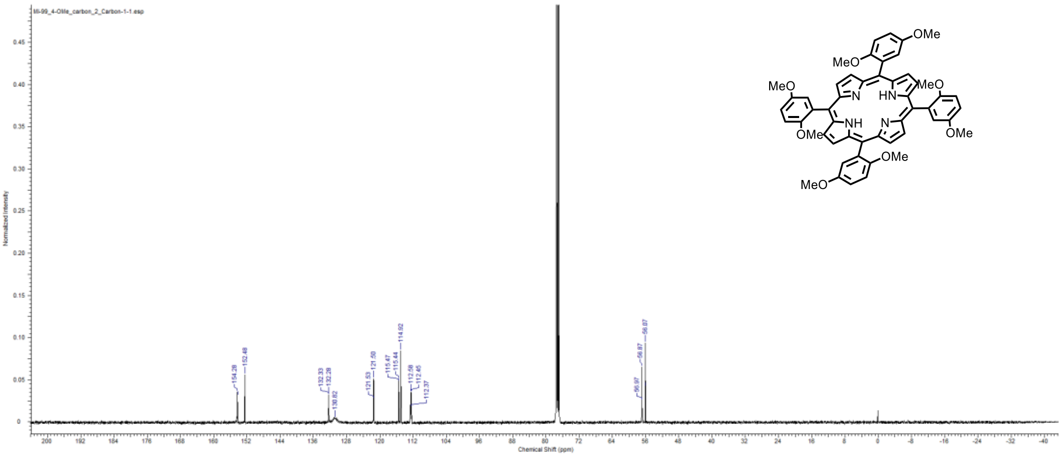

Fig. S7 ^{13}C NMR spectrum of **1’** in chloroform-*d*.

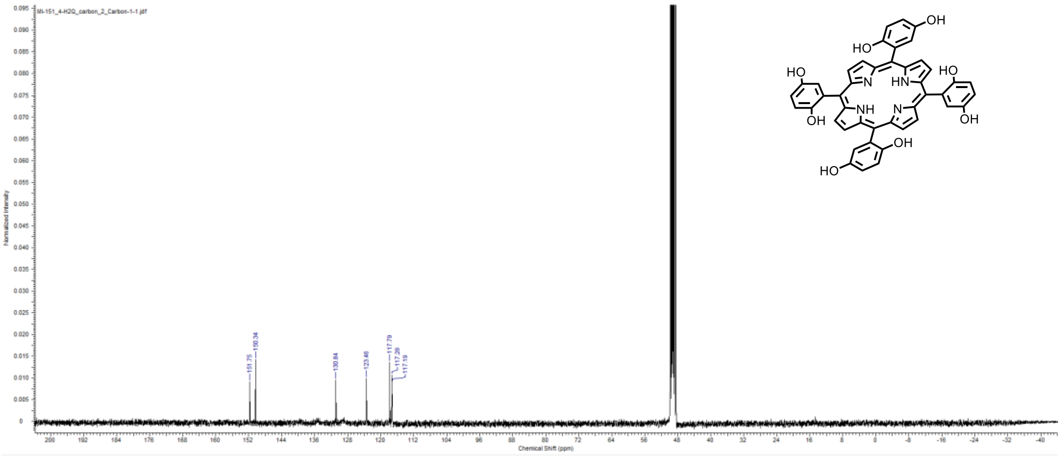

Fig. S8 ^{13}C NMR spectrum of **1** in methanol-d_4.

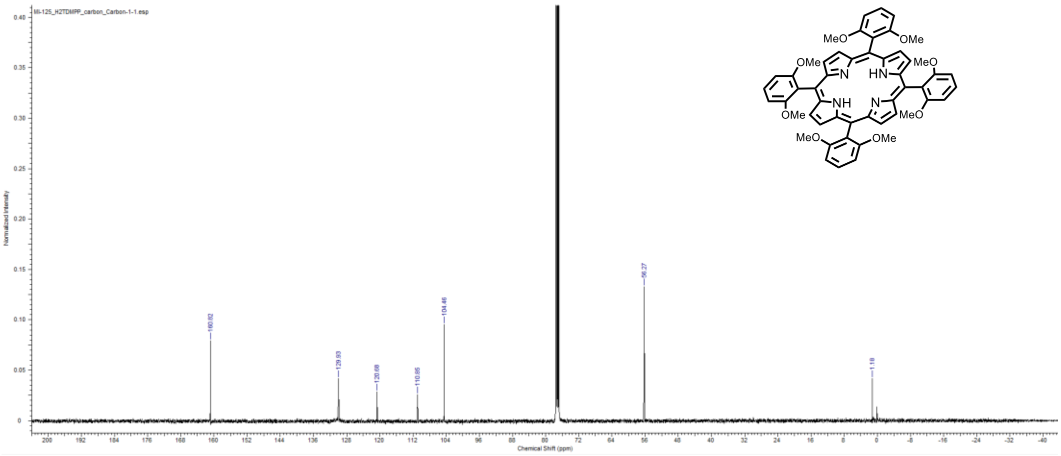

Fig. S9 ^{13}C NMR spectrum of **H$_2$TDMPP** in chloroform-d.

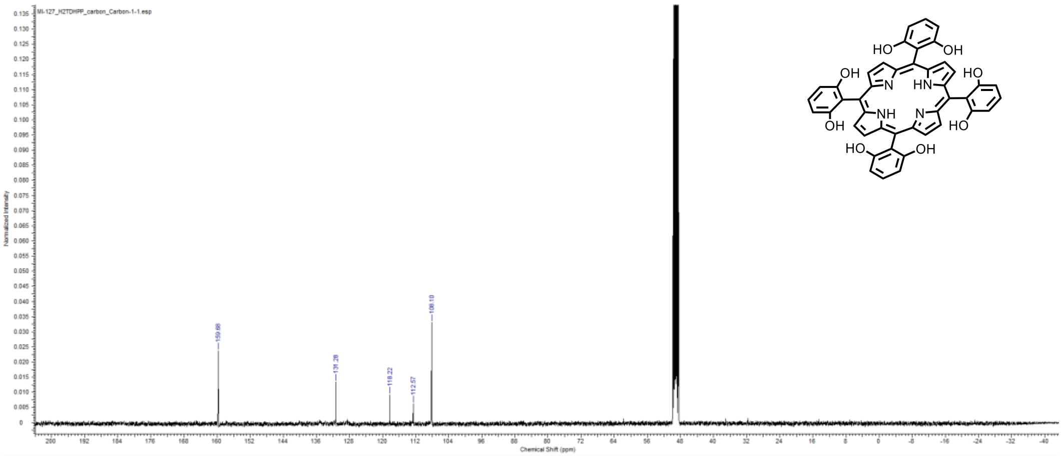

Fig. S10 ^{13}C NMR spectrum of **H$_2$TDHPP** in methanol-d_4.

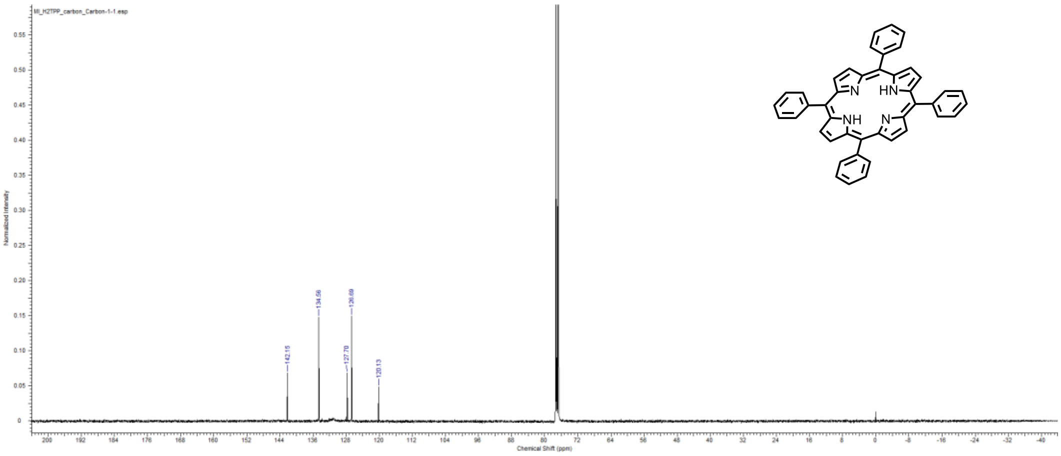

Fig. S11 ^{13}C NMR spectrum of **H$_2$TPP** in chloroform-*d*.

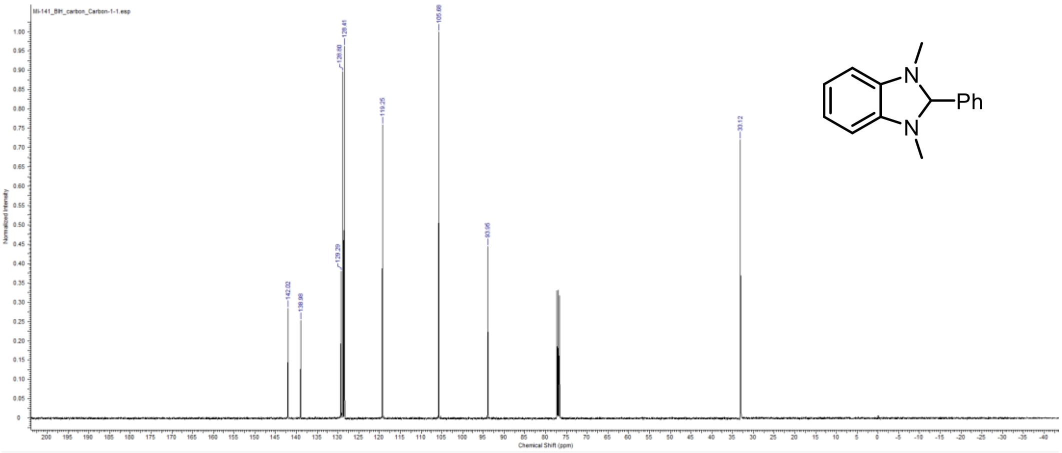

Fig. S12 ^{13}C NMR spectrum of BIH in chloroform-*d*.

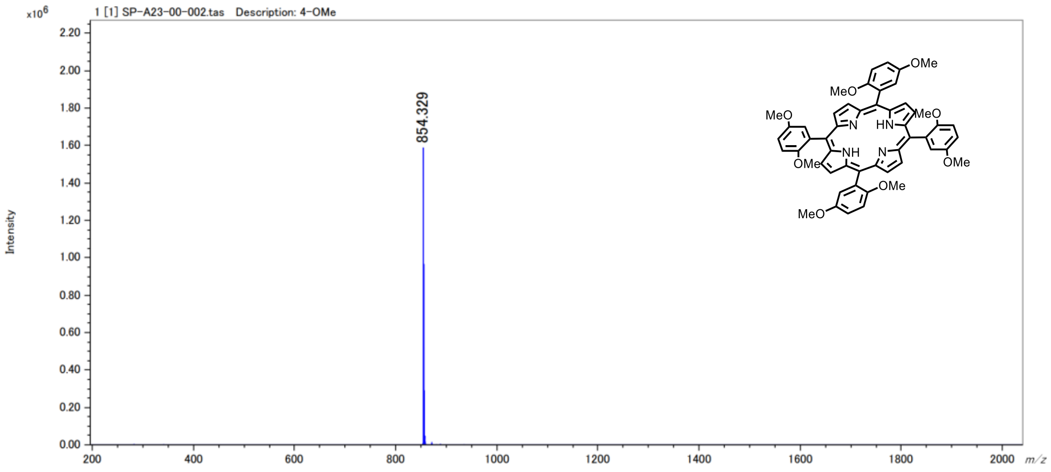

Fig. S13 MALDI spiral-TOF mass spectrum of **1’**.

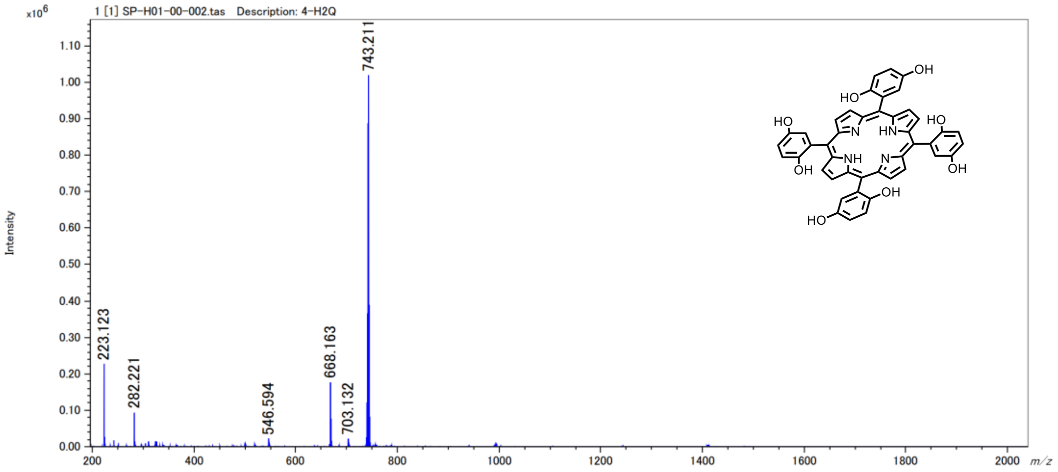

Fig. S14 MALDI spiral-TOF mass spectrum of **1**.

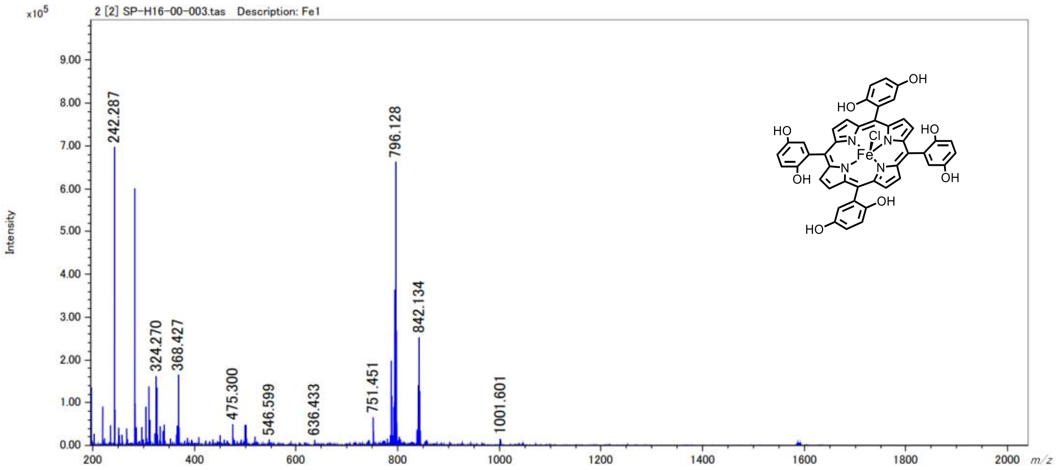

Fig. S15 MALDI spiral-TOF mass spectrum of **Fe1**.

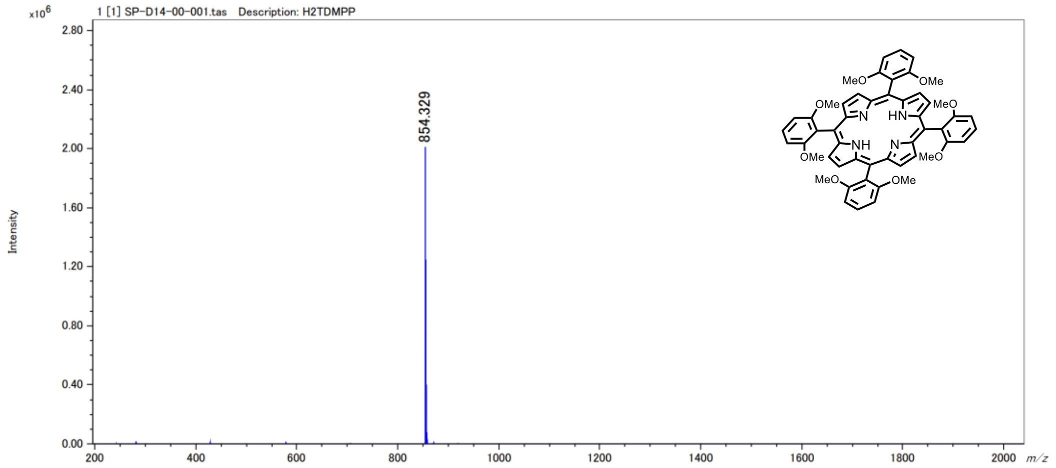

Fig. S16 MALDI spiral-TOF mass spectrum of **H_2TDMPP**.

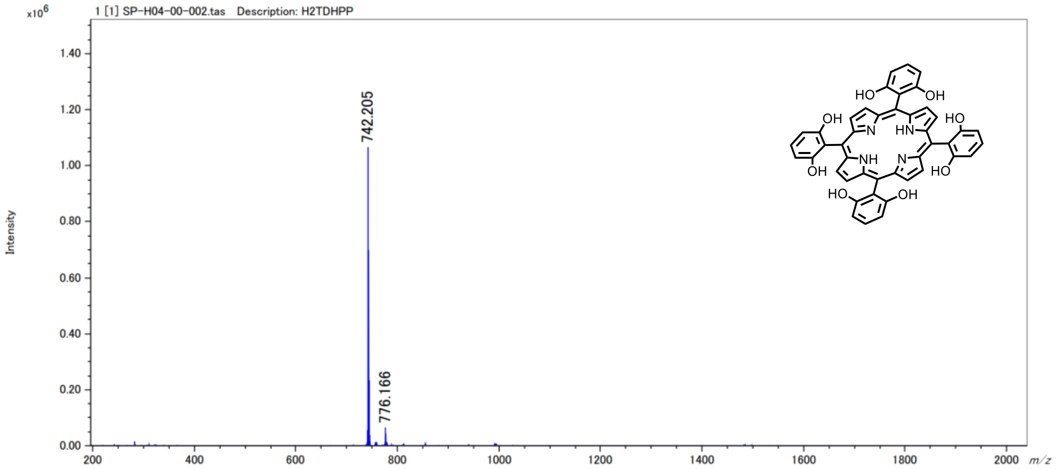

Fig. S17 MALDI spiral-TOF mass spectrum of **H_2TDHPP**.

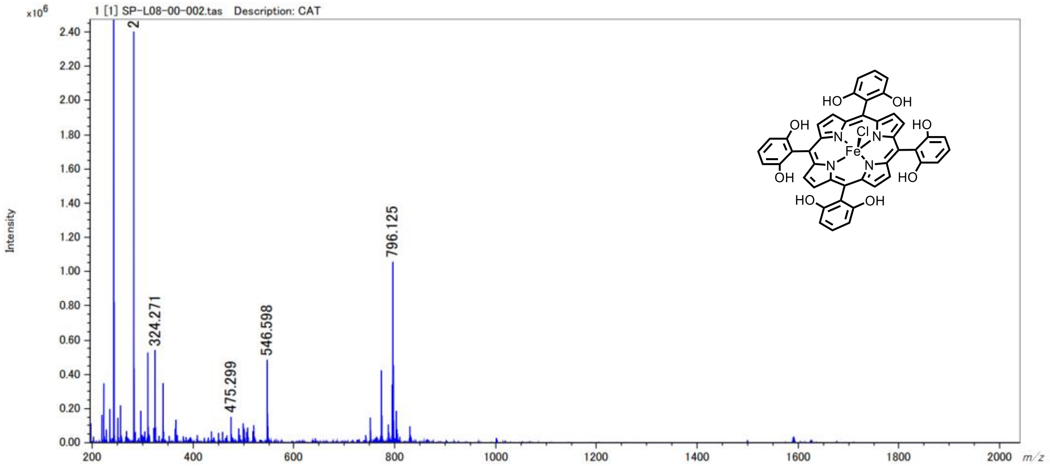

Fig. S18 MALDI spiral-TOF mass spectrum of **CAT**.

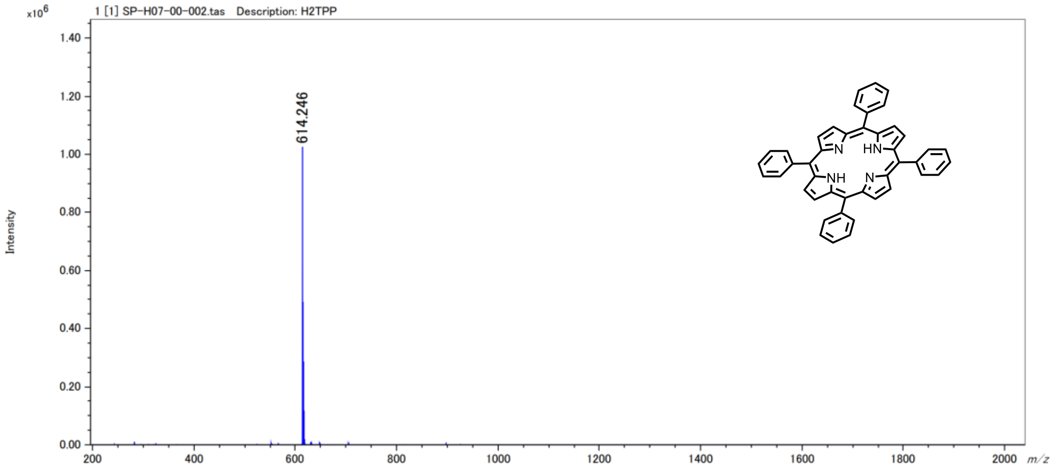

Fig. S19 MALDI spiral-TOF mass spectrum of **H_2TPP**.

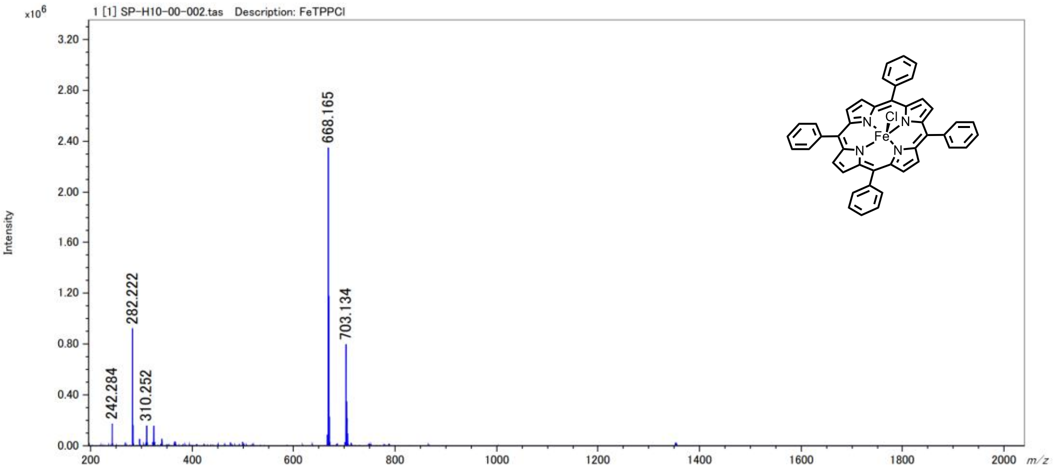

Fig. S20 MALDI spiral-TOF mass spectrum of **FeTPP-Cl**.

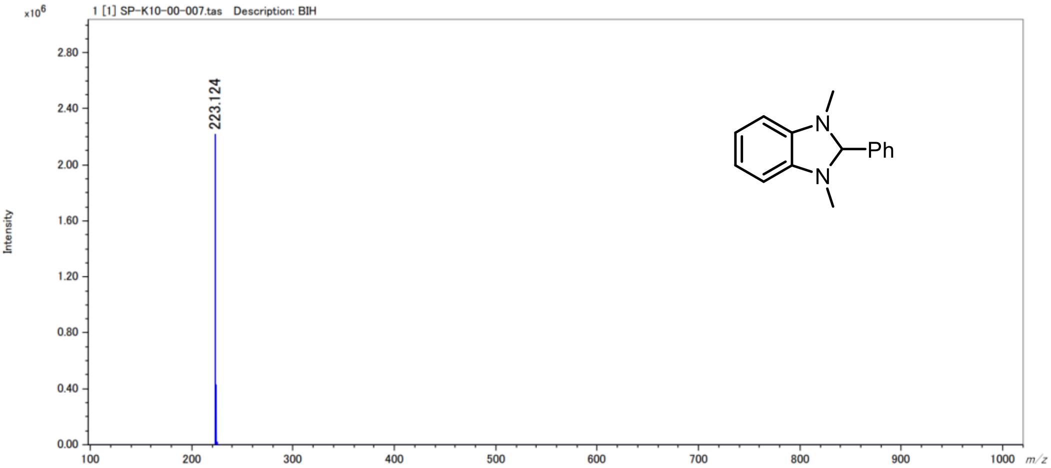

Fig. S21 MALDI spiral-TOF mass spectrum of BIH.

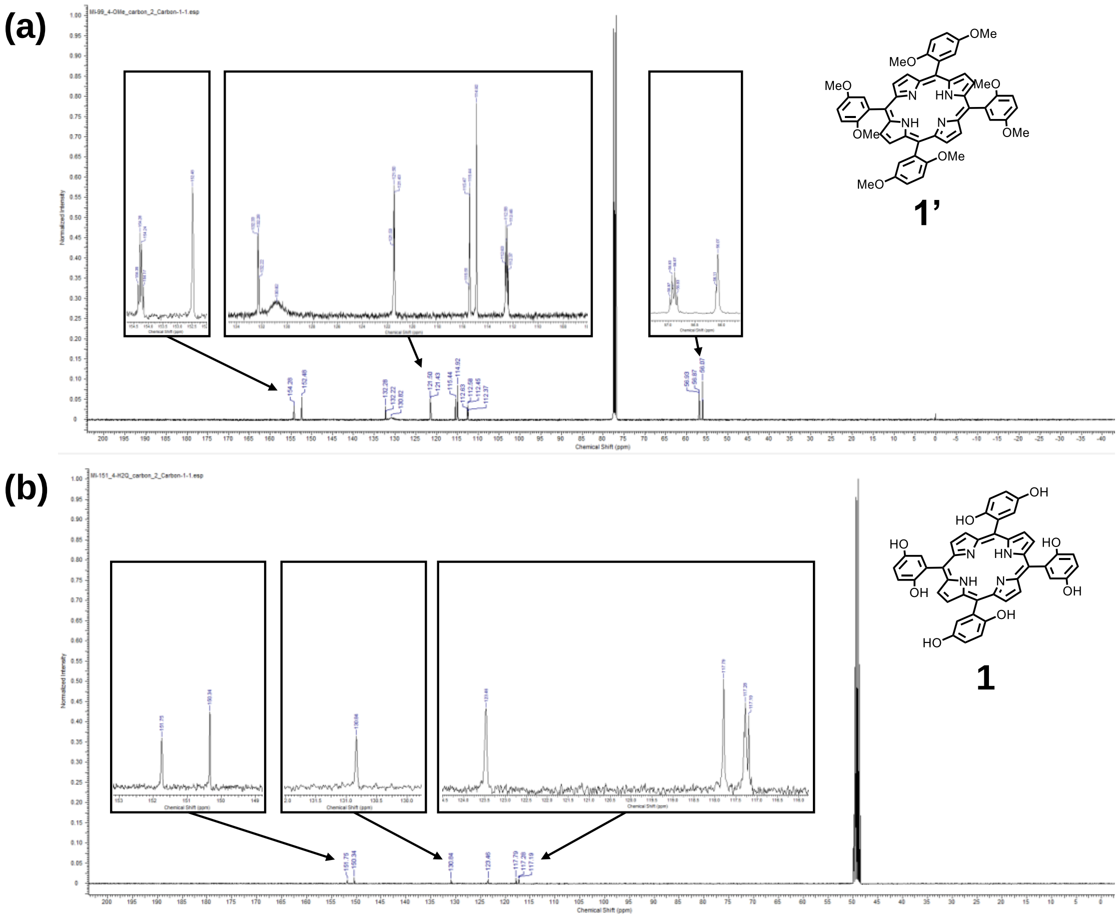

Fig. S22 ^{13}C NMR spectra of (a) **1'** in chloroform-*d* and (b) **1** in methanol-d_4 at 20 °C. In ^{13}C NMR spectrum of **1'**, many peaks were observed as multiplets, which indicates the existence of several atropisomers. On the other hand, in the spectrum of **1**, all the peaks are obtained as singlet peaks, indicating that the hydroquinone moieties freely rotate at 20 °C. Therefore, hydroquinone moieties of **Fe1** are indicated to freely rotate during photochemical reaction, and there are no distinguishable atropisomers.

Photochemistry

For typical run, a solution of MeCN (2.0 mL) containing 2.0 µM **Fe1**, 20 µM Ir(ppy)$_3$, 0.10 M BIH and 0.10 M TFE was purged with CO_2 for 15 minutes unless otherwise stated. The solution was then irradiated with a 150 W Xe lamp equipped with 400 nm long pass filter (Edmund Industrial Optics) to produce the light in the range of $400 \leq \lambda \leq 750$ nm at 20 ºC in a custom made aluminium box with cooling system. The amount of CO and H_2 produced at the headspace of the cell was quantified by a Shimadzu GC-8A with a TCD detector equipped with a packed column with Molecular Sieve 13X-S 60/80. Calibration curves were obtained by sampling known amounts of H_2 and CO.

$^{13}CO_2$ labeling experiment

A solution of MeCN (2.0 ml) containing 2.0 µM **Fe1**, 20 µM Ir(ppy)$_3$, 0.10 M BIH and 0.10 M TFE was purged with Ar for 15 min, followed by $^{13}CO_2$ bubbling for 5 min. The $^{13}CO_2$ gas was produced by adding 2.0 M HCl to solid Ba^{13}CO$_3$ (98 atom % ^{13}C, Sigma Aldrich). The evolved CO was detected by a GCMS-QP2020 (Rt®-Msieve 5A (30 m, 0.53 mm ID, 50 µm df) He carrier gas, 40 °C).

Electrochemistry

Electrochemical experiments were performed at room temperature on a BAS ALS Model 650DKMP electrochemical analyzer. Cyclic voltammetry (CV) measurements were performed by using a one-compartment cell with a three-electrode configuration, which consisted of a glassy carbon disk (diameter 3 mm, BAS Inc.), platinum wire, and Ag/Ag$^+$ electrode (Ag/0.01 M $AgNO_3$) as the working, auxiliary, and reference electrodes, respectively. The glassy carbon disc working electrode was polished using 0.05 µm alumina paste (from BAS Inc.) and washed with purified H_2O prior to each measurement. Ferrocene was used as an internal standard and all potentials are referenced to the ferrocenium/ferrocene (Fc/Fc$^+$) couple at 0 V.

2. UV-vis absorption spectroscopy

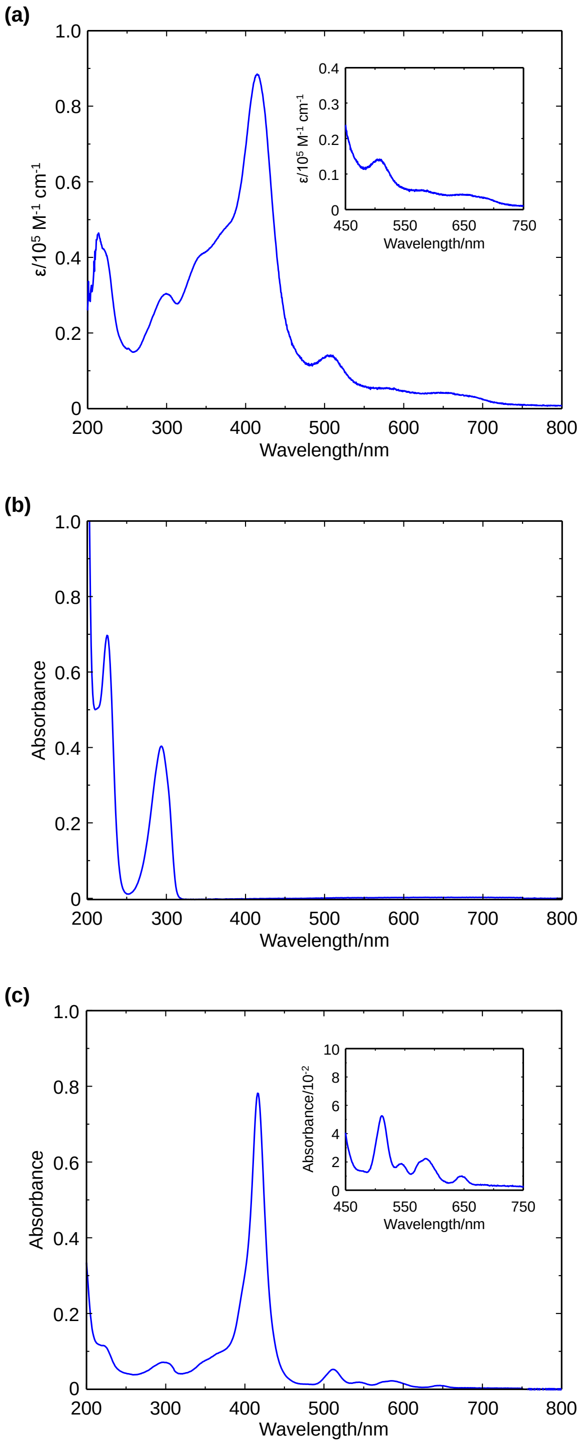

Fig. S23 UV-vis absorption spectra of (a) **Fe1**, (b) hydroquinone, and (c) **1** in MeCN. The insets exhibit the enlarged UV-vis absorption spectra at Q-bands region.

3. Electrochemical measurements

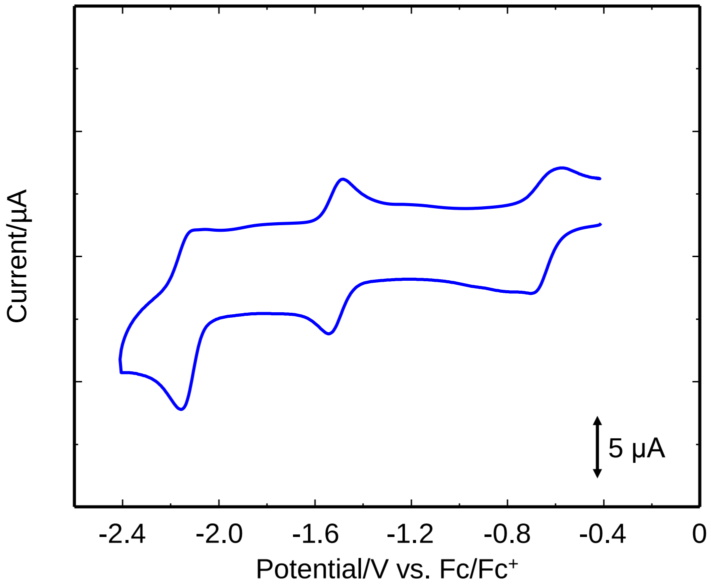

Fig. S24 Cyclic voltammogram of **FeTPP-Cl** (0.20 mM) in DMF with TBAP (0.1 M) under Ar (scan rate: 100 mV s^{-1}).

Table S1. Redox potentials of **Fe1**, **FeTPP-Cl**, and **CAT**.

Compound	$E_{1/2}(1)$	$E_{1/2}(2)$	$E_{1/2}(3)$
Fe1	−0.72	−1.60	−2.11
FeTPP-Cl	−0.64	−1.51	−2.13
CAT[a]	−0.84	−1.67	−2.11

[a] Reported values.[S6]

4. Photocatalytic activity for CO_2 reduction

All photocatalytic reactions were performed at 20 °C using a custom-made photoreactor with coolant to control the temperature of sample during photoreaction. The schematic illustration and photograph of the experimental setup are shown in Fig. S25.

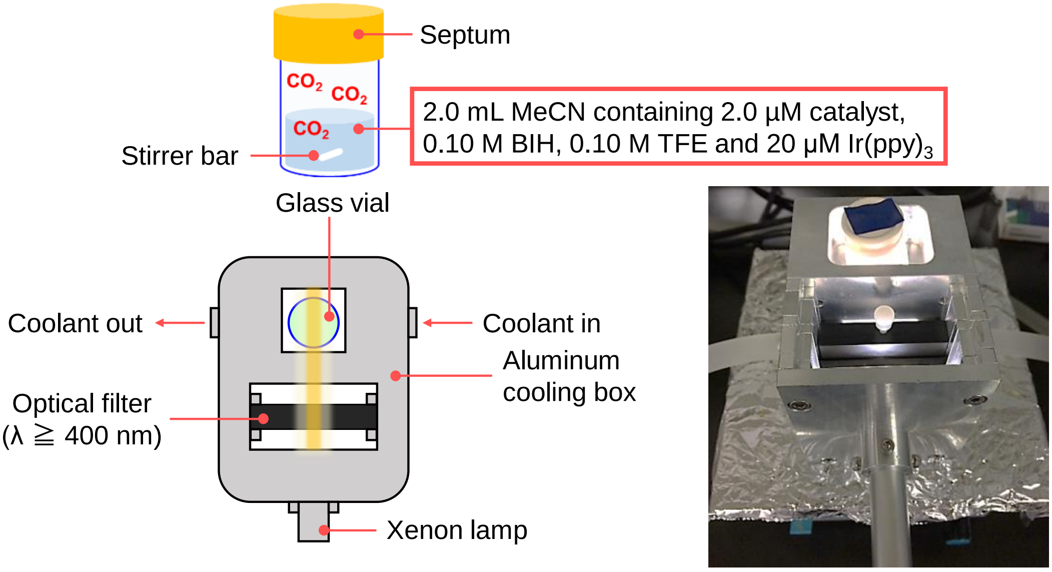

Top view

Actual view

Fig. S25 Custom-made photoreactor. Schematic illustration and a photograph are shown. The coolant was set to 20 °C to maintain a constant sample temperature during measurement.

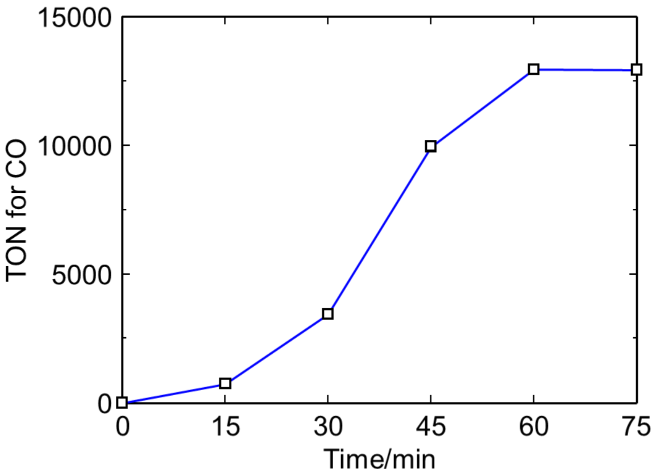

Fig. S26 Time course of CO production by **Fe1**. A CO_2-saturated MeCN solution containing 2.0 µM **Fe1**, 20 µM Ir(ppy)$_3$, 0.10 M BIH, and 0.10 M TFE was irradiated using a Xe lamp ($400 \leq \lambda \leq 750$ nm) at 20 °C.

Table S2. Photochemical CO_2 reduction by **Fe1** and **CAT** for 1 h.

Catalyst[a]	Photosensitiser[b]	Electron donor	Gas	Light[d]/nm	Media	TON	
						CO	H_2
Fe1	$Ir(ppy)_3$	BIH	CO_2	$400 \leq \lambda \leq 750$	0.10 M TFE/MeCN	1.3×10^4	0
CAT	$Ir(ppy)_3$	BIH	CO_2	$400 \leq \lambda \leq 750$	0.10 M TFE/MeCN	1.0×10^3	1[e]

[a] 2.0 µM of Catalyst [b] 20 µM $Ir(ppy)_3$ [c] 0.10 M BIH [d] Xe lamp (150 W) with long pass filter [e] Measured after 75 min of photoirradiation.

5. Quantum chemical calculation

Quantum chemical calculation was performed to determine the optimized structure of CO_2 adducts of the three electron-reduced species of **Fe1**. B3LYP[S7-S8] were used as a functional. Here, LANL2DZ (with core potential) basis set was used on iron, and 6-31G(*d*) basis set was used on the rest of the atoms (C, H, N and O). Solvation effects were included implicitly by the conductor-like polarizable continuum model (CPCM), with a dielectric constant mimicking MeCN.[S9] All calculations were performed with the Gaussian 16 program package.[S10]

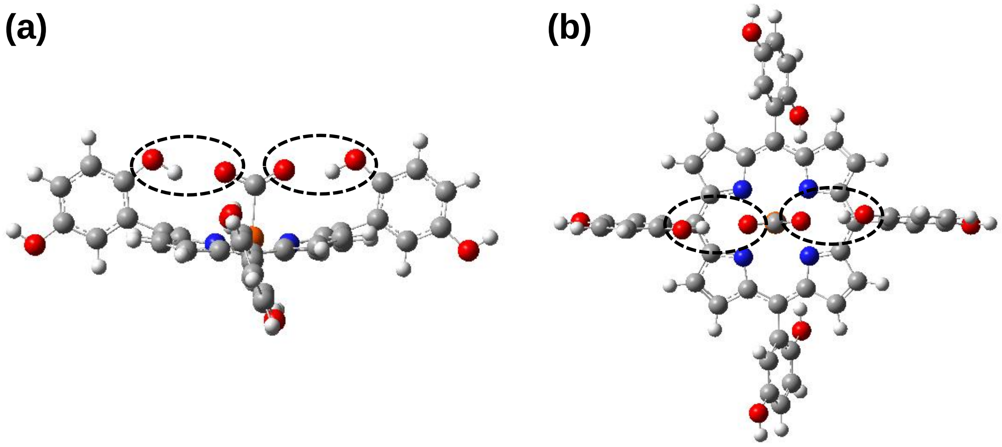

Fig. S27 Optimized structure of CO_2 adduct of the three electron-reduced species of **Fe1**. (a) Side view of **Fe1**. (b) Top view of **Fe1**. C = gray, H = white, N = blue and O = red, Fe = orange.

6. Emission quenching experiments

Samples for the quenching experiments were prepared in a 4 mL glass cuvette with a septum screw cap. In a typical experiment, the emission spectrum of a 10 μM solution of $Ir(ppy)_3$ in MeCN was collected. $Ir(ppy)_3$ was irradiated at 420 nm. Luminescence spectra were collected on Shimazu RF5300PC spectrofluorophotometer.

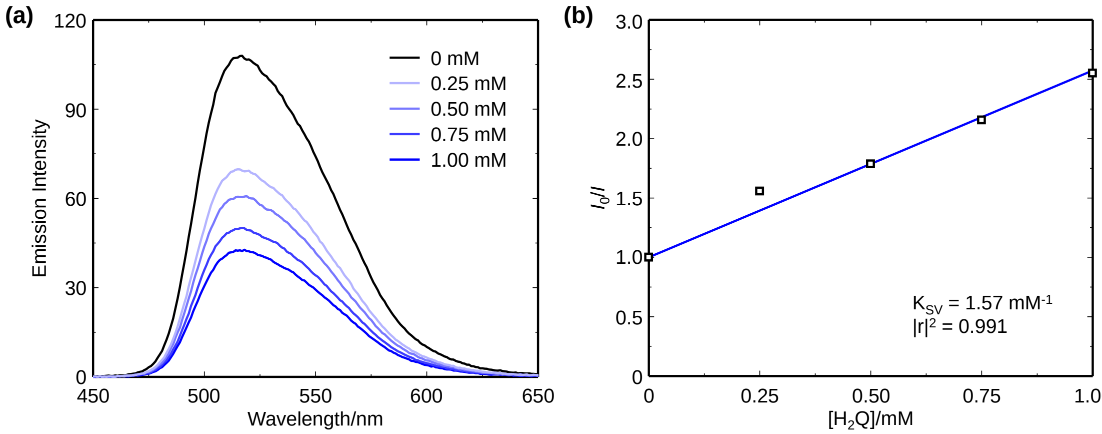

Fig. S28 (a) Emission spectra of 10 μM $Ir(ppy)_3$ upon increasing concentration of hydroquinone (H_2Q) and 1,8-diazabicyclo[5.4.0]-7-undecene (DBU) in MeCN under Ar after excitation at 420 nm ($[H_2Q]$ = [DBU]). (b) Results of Stern-Volmer analysis, where I_0/I is the emission intensity without quencher (I_0) divided by the emission intensity with a known concentration of quencher (I).

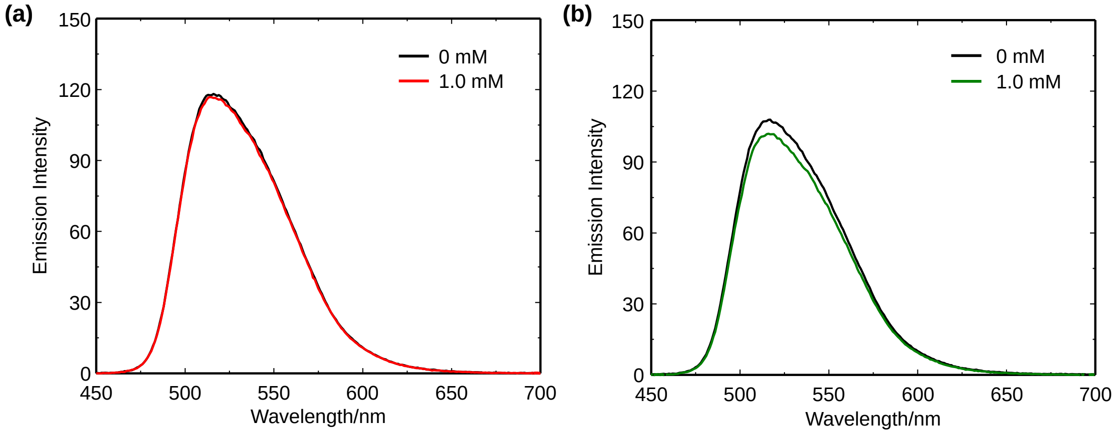

Fig. S29 Emission spectra of 10 μM $Ir(ppy)_3$ in the presence of (a) DBU and (b) H_2Q in MeCN under Ar after excitation at 420 nm.

7. Comparison of catalytic ability

Table S3. A comparison of TOFs of iron porphyrin complexes for photochemical CO_2 reduction.

Catalyst	Media	Electron donor	Photosensitizer	Light/nm	[a]TOF/h^{-1}	Ref.
Fe1 (2.0 μM)	MeCN/TFE	BIH	Ir(ppy)$_3$	$400 \leq \lambda \leq 750$	12954	**This work**
CAT (0.2 μM)	DMF	BIH	CuPP	$\lambda \geq 400$	7650	S11
FePor1 (0.2 μM)	DMF/H_2O	BIH	Ru(bpy)$_3^{2+}$	$\lambda = 460$	3720	S12
FePor2 (0.005 μM)	MeCN/H_2O	TEA	[Ir(ppy)$_2$bpy]PF$_6$	White LED	1375	S13
FePor3 (2 μM)	MeCN/H_2O	TEA	[Ir(ppy)$_2$bpy]PF$_6$	White LED	[b]71	S13
FePor4 (2 μM)	MeCN/H_2O	TEA	[Ir(ppy)$_2$bpy]PF$_6$	White LED	[b]68	S13
FePor5 (2 μM)	MeCN/H_2O	TEA	[Ir(ppy)$_2$bpy]PF$_6$	White LED	[b]57	S13
FePor6 (34 μM)	MeCN	TEA	p-terphenyl	$\lambda \geq 300$	[c]21	S14
FeTPP-Cl (100 μM)	MeCN	TEA	p-terphenyl	$\lambda \geq 300$	[c]14	S15
FePor3 (2 μM)	MeCN/TFE	TEA	Ir(ppy)$_3$	$\lambda \geq 420$	[b]5.1	S16
CAT (2 μM)	MeCN	TEA	Ir(ppy)$_3$	$\lambda \geq 420$	[b]2.5	S17

[a] The turnover frequency was calculated by dividing the turnover number with duration of photoirradiation. [b] The turnover frequency calculated from the numbers in the articles are listed. [c] The turnover frequency was calculated by dividing the approximate turnover number with duration of photoirradiation.

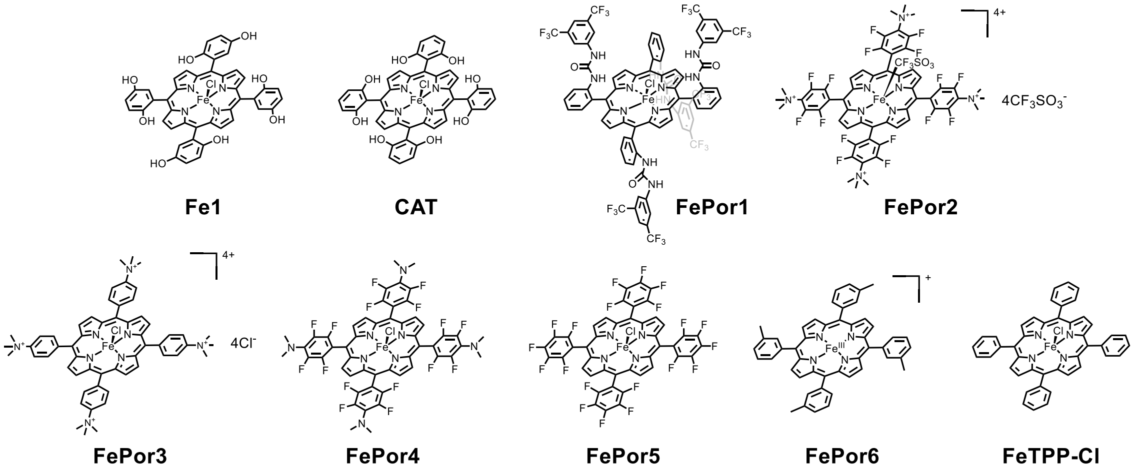

Fig. S30 Chemical structures of iron porphyrin complexes in Table S3.

Table S4. A comparison of TONs of iron-complex-based catalysts for photochemical CO_2 reduction.

Catalyst	Media	Electron donor	Photosensitizer	Light/nm	TON	Ref.
$[Fe(tpyPY2Me)]^{2+}$ (0.2 μM)	MeCN	BIH	$[Ru(bpy)_3]^{2+}$	$\lambda = 460$	30349 (45 min)	S18
CAT (0.2 μM)	DMF	BIH	CuPP	$\lambda \geq 400$	16109 (23 h)	S11
Fe_6L_6 (4 μM)	DMF/H_2O	TEA	4CzIPN	$420 \leq \lambda \leq 650$	14956 (2 h)	S19
$[Fe(qnpy)(H_2O)_2]^{2+}$ (5 μM)	$MeCN/H_2O$	BIH	$[Ru(phen)_3]^{2+}$	$\lambda = 460$ (centered at)	14095 (68 h)	S20
FePor1 (0.2 μM)	DMF/H_2O	BIH	$[Ru(bpy)_3]^{2+}$	$\lambda = 460$	13299 (2 h)	S12
Fe1 (2.0 μM)	MeCN/TFE	BIH	$Ir(ppy)_3$	$400 \leq \lambda \leq 750$	12954 (1 h)	**This work**
FeQPY (0.2 μM)	MeCN	BIH/TEOA	Al-4	$\lambda = 405$	10250 (4 h)	S21
$Fe(Ntpy)_2$ (10 μM)	DMF/H_2O	TEA	$[Ru(bpy)_3]^{2+}$	$420 \leq \lambda \leq 650$	6320 (2 h)	S22
FePor2 (0.005 μM)	$MeCN/H_2O$	TEA	$[Ir(ppy)_2bpy]PF_6$	White LED	5500 (4 h)	S13
$[Fe(qpy)(OH_2)_2]^{2+}$ (5 μM)	MeCN	BIH	$[Ru(bpy)_3]^{2+}$	$\lambda = 460$ (centered at)	3844 (45 min)	S23
FeTotpy (10 μM)	DMF/H_2O	TEA	4CzIPN	$420 \leq \lambda \leq 650$	2250 (3 h)	S24
FePB-2(P) (2 μM)	MeCN/TFE	BIH	$Ir(ppy)_3$	$\lambda = 440$	1168 (1 h)	S25
$Fe^{II}(dmp)_2(NCS)_2$ (50 μM)	MeCN	TEOA	Cu2Bph	$\lambda = 436$	778 (48 h)	S26
^{a}**[Fe]** (5 μM)	NMP	TEOA	$[Ir(dF(CF_3)ppy)_2(dtbbpy)](PF_6)$	$400 \leq \lambda \leq 700$	596 (5 h)	S27
$Fe(LN4H_2)Cl_2$ (25 μM)	DMF	TEOA	$[Cu(bathocuproine)(xantphos)](PF_6)$	$\lambda \geq 400$	565 (8 h)	S28
$[Fe(dqtpy)(H_2O)]^{2+}$ (50 μM)	DMF/TFE	BIH	PP	$\lambda = 460$ (centered at)	544 (15 h)	S29
^{a}**[Fe]** (133 μM)	NMP	BIH/TEOA	$[Cu(bathocuproine)(POP\text{-}xantphos)](PF_6)$	$400 \leq \lambda \leq 700$	505 (5 h)	S30
^{a}**[Fe]** (1 μM)	NMP	TEOA	Cu PS (generated *in situ*)	$400 \leq \lambda \leq 700$	487 (5 h)	S31
FePor3 (2 μM)	MeCN	TEA	$Ir(ppy)_3$	$\lambda \geq 420$	367 (102 h)	S16
FePor3 (2 μM)	$MeCN/H_2O$	TEA	$[Ir(ppy)_2bpy]PF_6$	White LED	282 (4 h)	S13
$Fe^{II}(dmp)_2(NCS)_2$ (50 μM)	MeCN	TEOA	$([Cu^I\{P_2baphen\}]_2^{2+}(PF_6^-)_2$	$\lambda = 436$	273 (12 h)	S32
FePor4 (2 μM)	$MeCN/H_2O$	TEA	$[Ir(ppy)_2bpy]PF_6$	White LED	272 (4 h)	S13
FePor5 (2 μM)	$MeCN/H_2O$	TEA	$[Ir(ppy)_2bpy]PF_6$	White LED	226 (4 h)	S13
CAT (2 μM)	MeCN	TEA	$Ir(ppy)_3$	$\lambda \geq 420$	140 (55 h)	S17

Table S4. Continued.

Catalyst	Media	Electron donor	Photosensitizer	Light/nm	TON	Ref.
FePor6 (34 µM)	MeCN	TEA	p-terphenyl	$\lambda \geq 300$	^{b}63 (21 h)	S14
ClFe(tdcc) (45 µM)	MeCN	TEA	p-terphenyl	$\lambda \geq 310$	^{b}50 (4 h)	S33
ClFe(tpfc) (48 µM)	MeCN	TEA	p-terphenyl	$\lambda \geq 310$	^{b}46 (8.2 h)	S33
FeTPP-Cl (100 µM)	MeCN	TEA	p-terphenyl	$\lambda \geq 300$	^{b}20 (3 h)	S15

[a] **[Fe]** = Iron, tricarbonyl[(1,3,3a,7a-η)-4,5,6,7-tetrahydro-1,3-bis(trimethylsilyl)-2*H*-inden-2-one]-. [b] The approximate turnover number from the figures in the articles are listed.

8. References

S1. C. Costentin, S. Drouet, M. Robert and J. M. Savéant, *Science*, **2012**, *338*, 90.

S2. P. Bhyrappa, S. R. Wilson and K. S. Suslick, *J. Am. Chem. Soc.*, **1997**, *119*, 8492.

S3. A. D. Alder, F. R. Long, W. Shergalis, *J. Am. Chem. Soc.,* **1964**, *86*, 3145.

S4. S. L. Rebelo, A. M. N. Silva, C. J. Medforth, C. Freire, *Molecules*, **2016**, *21*, 481.

S5. R. N. Sampaio, D. C. Grills, D. E. Polyansky, D. J. Szalda and E. Fujita, *J. Am. Chem. Soc.*, **2020**, *142*, 2413.

S6. A. Sonea, K. L. Branch and J. J. Warren, *ACS Catal.*, **2023**, *13*, 3902.

S7. A. D. Becke, *J. Chem. Phys.*, **1993**, *98*, 5648.

S8. C. Lee, W. Yang and R. G. Parr, *Phys. Rev. B.*, **1988**, *37*, 785.

S9. J. Tomasi, B. Mennucci and R. Cammi, *Chem. Rev.*, **2005**, *105*, 2999.

S10. Gaussian 16, Revision C.01, M. J. Frisch, G. W. Trucks, H. B. Schlegel, G. E. Scuseria, M. A. Robb, J. R. Cheeseman, G. Scalmani, V. Barone, G. A. Petersson, H. Nakatsuji, X. Li, M. Caricato, A. V. Marenich, J. Bloino, B. G. Janesko, R. Gomperts, B. Mennucci, H. P. Hratchian, J. V. Ortiz, A. F. Izmaylov, J. L. Sonnenberg, D. Williams-Young, F. Ding, F. Lipparini, F. Egidi, J. Goings, B. Peng, A. Petrone, T. Henderson, D. Ranasinghe, V. G. Zakrzewski, J. Gao, N. Rega, G. Zheng, W. Liang, M. Hada, M. Ehara, K. Toyota, R. Fukuda, J. Hasegawa, M. Ishida, T. Nakajima, Y. Honda, O. Kitao, H. Nakai, T. Vreven, K. Throssell, J. A. Montgomery, Jr., J. E. Peralta, F. Ogliaro, M. J. Bearpark, J. J. Heyd, E. N. Brothers, K. N. Kudin, V. N. Staroverov, T. A. Keith, R. Kobayashi, J. Normand, K. Raghavachari, A. P. Rendell, J. C. Burant, S. S. Iyengar, J. Tomasi, M. Cossi, J. M. Millam, M. Klene, C. Adamo, R. Cammi, J. W. Ochterski, R. L. Martin, K. Morokuma, O. Farkas, J. B. Foresman, and D. J. Fox, Gaussian, Inc., Wallingford CT, 2016.

S11. H. Yuan, B. Cheng, J. Lei, L. Jiang and Z. Han, *Nat. Commun.*, **2021**, *12*, 1835.

S12. E. Pugliese, P. Gotico, I. Wehrung, B. Boitrel, A. Quaranta, M. H. Ha-Thi, T. Pino, M. Sircoglou, W. Leibl, Z. Halime and A. Aukauloo, *Angew. Chem. Int. Ed.*, **2022**, *61*, e202117530.

S13. A. Stoumpidi, A. Trapali, M. Poisson, A. Barrozo, S. Bertaina, M. Orio, G. Charalambidis and A. G. Coutsolelos, *ChemCatChem*, **2023**, *15*, e202200856.

S14. J. Grodkowski and P. Neta, *J. Phys. Chem. A*, **2000**, *104*, 4475.

S15. T. Dhanasekaran, J. Grodkowski, P. Neta, P. Hambright and E. Fujita, *J. Phys. Chem. A*. **1999**, *103*, 7742.

S16. H. Rao, L. C. Schmidt, J. Bonin and M. Robert, *Nature*, **2017**, *548*, 74.

S17. J. Bonin, M. Robert and M. Routier, *J. Am. Chem. Soc.*, **2014**, *136*, 16768.

S18. P. De La Torre, J. S. Derrick, A. Snider, P. T. Smith, M. Loipersberger, M. Head-Gordon and C. J. Chang, *ACS Catal.*, **2022**, *12*, 8484.

S19. Y. Wang, L. Chen, T. Liu and D. Chao, *Dalton Trans.*, **2021**, *50*, 6273.

S20. Y. Qin, L. Chen, G. Chen, Z. Guo, L. Wang, H. Fan, M. Robert and T.-C. Lau, *Chem. Commun.*, **2020**, *56*, 6249.

S21. J.-W. Wang, F. Ma, T. Jin, P. He, Z.-M. Luo, S. Kupfer, M. Karnahl, F. Zhao, Z. Xu, T. Jin, T. Lian, Y.-L. Huang, L. Jiang, L.-Z. Fu, G. Ouyang and X.-Y. Yi, *J. Am. Chem. Soc.*, **2023**, *145*, 676.

S22. Y. Wang, T. Liu, L. Chen and D. Chao, *Inorg. Chem.*, **2021**, *60*, 5590.

S23. Z. Guo, S. Cheng, C. Cometto, E. Anxolabéhère-Mallart, S.-M. Ng, C.-C. Ko, G. Liu, L. Chen, M. Robert and T.-C. Lau, *J. Am. Chem. Soc.*, **2016**, *138*, 9413.

S24. Y. Wang, X.-W. Gao, J. Li and D. Chao, *Chem. Commun.*, **2020**, *56*, 12170.

S25. L. An, P. De La Torre, P. T. Smith, M. R. Narouz and C. J. Chang, *Angew. Chem. Int. Ed.*, **2023**, *62*, e202209396.

S26. H. Takeda, Y. Monma and O. Ishitani, *ACS Catal.*, **2021**, *11*, 11973.

S27. A. Rosas-Hernández, P. G. Alsabeh, E. Barsch, H. Junge, R. Ludwigab and M. Beller, *Chem. Commun.*, **2016**, *52*, 8393.

S28. Y. Sakaguchi, A. Call, M. Cibian, K. Yamauchi and K. Sakai, *Chem. Commun.*, **2019**, *55*, 8552.

S29. L. Chen, Y. Qin, G. Chen, M. Li, L. Cai, Y. Qiu, H. Fan, M. Robert and T.-C. Lau, *Dalton Trans.*, **2019**, *48*, 9596.

S30. P. A. Forero-Cortés, M. Marx, N. G. Moustakas, F. Brunner, C. E. Housecroft, E. C. Constable, H. Junge, M. Beller and J. Strunk, *Green Chem.*, **2020**, *22*, 4541.

S31. A. Rosas-Hernández, C. Steinlechner, H. Junge and M. Beller, *Green Chem.*, **2017**, *19*, 2356.

S32. H. Takeda, K. Ohashi, A. Sekine and O. Ishitani, *J. Am. Chem. Soc.*, **2016**, *138*, 4354.

S33. J. Grodkowski, P. Neta, E. Fujita, A. Mahammed, L. Simkhovich and Z. Gross, *J. Phys. Chem. A*, **2002**, *106*, 4772.